Close-range optical measurement of aircraft's 3D attitude and accuracy evaluation

Zhe Li (李 喆), Zhenliang Ding (丁振良), and Feng Yuan (袁 峰)

Department of Automatic Measurement and Control, Harbin Institute of Technology, Harbin 150001

Received December 11, 2007

A new screen-spot imaging method based on optical measurement is proposed, which is applicable to the close-range measurement of aircraft's three-dimensional (3D) attitude parameters. Laser tracker is used to finish the global calibrations of the high-speed cameras and the fixed screens on test site, as well as to establish media-coordinate-frames among various coordinate systems. The laser cooperation object mounted on the aircraft surface projects laser beams on the screens and the high-speed cameras synchronously record the light-spots' position changing with aircraft attitude. The recorded image sequences are used to compute the aircraft attitude parameters. Based on the matrix analysis, the error sources of the measurement accuracy are analyzed, and the maximum relative error of this mathematical model is estimated. The experimental result shows that this method effectively makes the change of aircraft position distinguishable, and the error of this method is no more than $3'$ while the rotation angles of three axes are within a certain range.

OCIS codes: 120.0120, 120.4640, 120.4820, 140.3460.
doi: 10.3788/COL20080608.0564.

The aircraft's three-dimensional (3D) attitude parameters are essential for reflecting the aircraft's flight conditions in ground test, and remarkable for various aspects, e.g., the aircraft's test evaluation, accident analysis, structural design, etc. As a measurement method of motion parameters, optional measurement has various features such as non-contact, full-field, and high accuracy, which make it a most common external method in target measurements[1,2].

There are various analysis and process methods currently, among which the axis joint method[3], feature point method[4,5], and profile matching method[6,7] are most commonly used. The feature point method and image matching method have higher accuracy of 0.2° and 0.1° respectively, and both are more precise than the axis joint method. However, feature points are easily interfered by the light emitted from the gas and flame discharged from the object during its movement, and may cause the images invalid. As to the profile matching method, it requires an aircraft model in advance, besides, quantity of data and calculation may be tremendous.

Considering the aforementioned issues, a mathematical model of the light spot imaging method based on image sequences is presented. Lasers installed on the surface of aircraft can project laser beams to the fixed screens on the test site, and those laser beams can form light-spots while the aircraft is in movement. Thus the flight attitude can be amplified to improve the accuracy of attitude measurement. Meanwhile, the high-speed cameras located in the test site can capture the position variation of those light spots, and then analyze the position variation recorded in image sequences to determine the aircraft's external attitude.

The measuring system consists of multiple high-speed cameras, laser tracker, projection screens, and laser cooperative target, as shown in Fig. 1. The laser cooperative target mounted on the aircraft's surface is made up of four high-power laser generators. The relative positions of laser generators are fixed, every two of them are coplanar and form guiding beams in "X" shape, and the guiding beams project four light-spots on the screens at each side where the position of light spot can change along with the changing of the aircraft's angular variation. Several multi-directional high-speed cameras are installed at the test site, and under the control of real-time bus the cameras synchronously capture the movement of light-spots and then save image sequences to high-speed disk arrays. The system has multiple coordinate systems, i.e., ground coordinate system $O_gX_gY_gZ_g$, screen coordinate system $O_hX_hY_hZ_h$, aircraft coordinate system $O_mX_mY_mZ_m$, and camera coordinate system $O_c^iX_c^iY_c^iZ_c^i$. The laser tracker is fixed on the test site, and it will be used to measure various parts of the system as well as confirm the above mentioned coordinate systems before the experiment. In post analysis and process, using transition matrix in various coordinate systems to unify the positions of light spots at each moment in one coordinate system, then it will be able to get the aircraft's various attitude parameters.

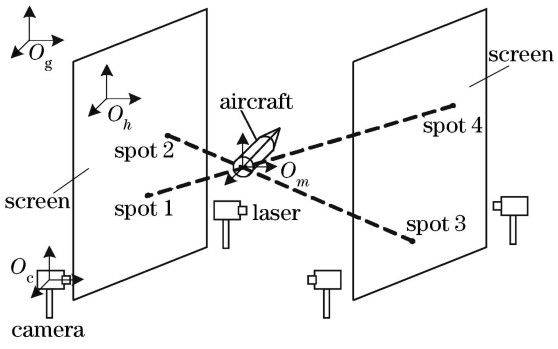

Fig. 1. Arrangement in test site.

If two coordinate systems $O_aX_aY_aZ_a$ and $O_bX_bY_bZ_b$ respectively rotate with angles ψ, θ, ϕ around present O_aZ_a, O_aY_a, and O_aX_a, then these two frames will completely coincide with each other. According to this principle, the coordinate transformation matrix between two coordinate systems is[8]

$$C_{ab} = \begin{bmatrix} \cos\theta\cos\psi & -\cos\phi\sin\psi+\sin\theta\sin\phi\cos\psi & \sin\theta\cos\phi\cos\psi+\sin\phi\sin\psi \\ \cos\theta\sin\psi & \sin\theta\sin\phi\sin\psi+\cos\phi\cos\psi & -\sin\phi\cos\psi+\sin\theta\cos\phi\sin\psi \\ -\sin\theta & \cos\theta\sin\phi & \cos\theta\cos\phi \end{bmatrix}. \tag{1}$$

When the laser cooperative target installed on the surface of aircraft begins to work, four light spots will appear on the screens at both sides of the test site, and the coordinates of those light spots in $O_mX_mY_mZ_m$ are $X_{mi} = (x_{mi}, y_{mi}, z_{mi})^{\mathrm{T}}$ $(i = 1, 2, 3, 4)$, in which the light spots 1 and 4 are collinear while the light spots 2 and 3 are collinear. The laser position matrix in $O_mX_mY_mZ_m$ can be expressed as[9]

$$D_{m0} = (A_{m14}, A_{m23}, B_m), \tag{2}$$

where $A_{m14} = (X_{m1} - X_{m4})/|X_{m1} - X_{m4}|$,
$A_{m23} = (X_{m2} - X_{m3})/|X_{m2} - X_{m3}|$,
$B_m = (A_{m14} \times A_{m23})/|A_{m14} - A_{m23}|$.

Also, after the aircraft rotates a certain angle around each axis, positions of the light spots on screen will change into $X'_{mi} = (x'_{mi}, y'_{mi}, z'_{mi})^{\mathrm{T}}$ $(i = 1, 2, 3, 4)$, and then we can get the attitude matrix $D_{mt} = (A'_{m14}, A'_{m23}, B'_m)$ for this moment. Then we can get the transition matrix under $O_mX_mY_mZ_m$:

$$C_m = D_{mt} \cdot D_{m0}^{-1}. \tag{3}$$

We can get each axis' angle of rotation by substituting it into Eq. (1).

To unify the coordinates of captured light spots into the ground coordinate system, and to guarantee the whole system's accuracy of measurement, it is necessary to calibrate cameras, screens, and the position of aircraft in the system, and further get the transition matrix of positions among coordinate systems. The laser tracker is applied for establishing $O_{\mathrm{g}}X_{\mathrm{g}}Y_{\mathrm{g}}Z_{\mathrm{g}}$ and $O_mX_mY_mZ_m$. It scans the screens at both sides. Then the built-in software of the laser tracker is used to process measuring results by least squares fitting to get the reference plane of measurement. The next step would be establishing $O_hX_hY_hZ_h$ on that reference plane. Coplanar spots should be properly set up on both screens as the calibration spots for cameras. The indicating light spots generated by laser tracker will locate those calibration spots, and then images of those light spots will be captured by the cameras in the system. Image sequences will be analyzed to get indicating light spot's position in each camera coordinate system $O_{\mathrm{c}}^iX_{\mathrm{c}}^iY_{\mathrm{c}}^iZ_{\mathrm{c}}^i$ to calibrate each camera respectively[10], then each camera's internal parameters and the rotary matrix R_{c} and translational vector T_{c} can be acquired. The transformation relation between each coordinate system can be written as

$$X_m = C_{ch} \cdot C_{hg} \cdot C_{gm} \cdot X_{\mathrm{c}}, \tag{4}$$

where X_m refers to light spot's coordinates in $O_mX_mY_mZ_m$, while X_{c} refers to light spot's coordinates in $O_{\mathrm{c}}^iX_{\mathrm{c}}^iY_{\mathrm{c}}^iZ_{\mathrm{c}}^i$, C_{ch}, C_{hg}, and C_{gm} respectively refer to the transition matrices between $O_{\mathrm{c}}^iX_{\mathrm{c}}^iY_{\mathrm{c}}^iZ_{\mathrm{c}}^i$, $O_hX_hY_hZ_h$, $O_{\mathrm{g}}X_{\mathrm{g}}Y_{\mathrm{g}}Z_{\mathrm{g}}$, and $O_mX_mY_mZ_m$. Thus, the relations between various parts in the system get unified after such global calibration, which further guarantees the accuracy of measurement of calculating method[11,12].

By analyzing the aforementioned mathematical model and principles of measurement, it can be deduced that the final accuracy of this measurement method relies on the precision of attitude matrix D_{m0} and D_{mt}. The critical factor which may affect the precision would be the position error of light spots analyzed as follows.

The first factor in position error is the straightness error of cooperative target's laser beam. Figure 2 indicates that the laser beams generated by the two opposite lasers cannot perfectly coincide with each other due to the installation error of those lasers, and certain angle will be formed instead. Therefore, there will be certain error in the position of light spots after the cooperative target rotate certain angle with the aircraft.

In the following calculation, the horizontal direction is used for example, and the angle between two laser beams is assumed to be $\Delta\theta$. At the initial position, the angles between laser beams and the horizontal direction are α and $\alpha + \Delta\theta$ respectively, and the angle between the horizontal direction and the vector formed by two light spots can be expressed as

$$y_1 = (l - s) \cdot \tan(\alpha + \Delta\theta), \quad y'_1 = (l + s) \cdot \tan\alpha,$$

$$\theta_1 = \arctan[(y_1 + y'_1/l)], \qquad \Delta l = |l - 2s|,$$

where Δl is the position of the target rotation center, and the other parameters are defined in Fig. 2. When the straight laser beam rotates for an angle β around the rotation center O, the angle between the vector and horizontal direction would be

$$y_2 = (l - s) \cdot \tan(\alpha + \Delta\theta + \beta),$$

$$y'_2 = (l + s) \cdot \tan(\alpha + \beta), \quad \theta_2 = \arctan[(y_2 + y'_2/l)].$$

Thus, a single light spot's position error caused by the straightness error of laser beam would be

$$\Delta\delta_l = \frac{1}{2}\frac{l}{\cos\theta_2} \cdot \tan(\theta_2 - \beta - \theta_1). \tag{5}$$

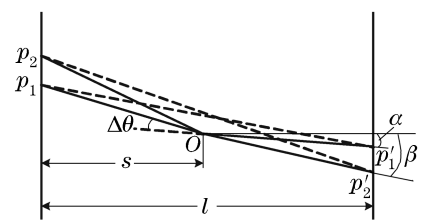

Fig. 2. Effect of straightness error of laser beams on light spots' position.

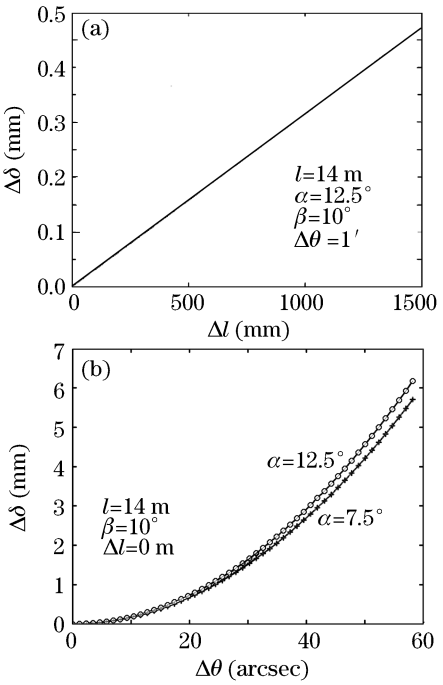

Fig. 3. Influence of straightness error of laser beams on light spots' position. (a) Effect of the cooperation object's rotation center and (b) effect of the laser beams straightness error.

Figure 3 shows the error caused by the straightness error of laser beam on light spot's location. It can be noticed that the position of a target rotation center has more influence on the position of light spots than any other factors, and the straightness error of laser beam will be amplified when the rotation center's position is getting away from the center of test site. So it is necessary to reasonably arrange the test site in advance. Reducing the angle between laser beam and horizontal direction can also relatively reduce such error, however, this may reduce the method's amplification on movement as well.

The second factor is the calibration error of each camera and screen in the system. According to the evaluation method for calibration errors given in Ref. [13], it can be confirmed that the maximum error of light spots caused by calibration error should be

$$\delta_{\rm c} \le \left[\left(1+\frac{1}{\sqrt{6N_0N_f}}\right)\frac{z}{f}+\frac{\|T_s\|}{L\sqrt{6N_0}}\left(1+\frac{1}{N_f}\right)+\frac{1}{2\sqrt{6N_0}}+\frac{1}{2\sqrt{6N_0}}\frac{z}{f}\right]\frac{z}{\|T_s\|}\cdot\delta+\Delta q, \tag{6}$$

where N_0 is the number of calibration points, N_f is the number of planes, f represents the object distance of lens, $\|T_s\|$ refers to the average distance between the cameras at all the calibration points, L is the calibration extent that can be captured by cameras, z is the distance between light spot to imaging plane, δ is the calculation error of the real position of calibration points. Δq is the position error of calibration centers, which is usually caused by the measurement error of laser tracker and the flatness error of screens. Its value can be expressed as

$$\Delta q=\sqrt{(l\cdot\tan\Delta\theta_s)^2+(\delta_s\cdot\tan\theta_c)^2},$$

where l is the average distance from the laser tracker to screens, $\Delta\theta_s$ is the angular resolution of laser tracker, δ_s is the flatness error of screens, θ_c is the angle between the optical axis of cameras and screens. From Eq. (6), it can be noticed that Δq and δ are key factors in camera calibration, and the influence of calibration error on measurement accuracy will be less significant when there are certain number of calibration points.

The third factor is the influence from the smearing caused by the movement of light spots when they are captured by cameras. Considering that the movement of aircraft is amplified in this model, the movement speed of light spots on screens is therefore amplified as well when the aircraft moves with high speed, which causes smearing in the captured image, and further influences the center of light spots. Assumed that the exposure duration of a camera is t, and the aircraft's angular speed at single direction is ω, then the error of a light spot's center during shooting would be

$$\delta_t=\frac{1}{2}\cdot\tan(\omega\cdot t)\cdot\left(\frac{l}{2}+s\right)\Big/\cos(\alpha+\beta). \tag{7}$$

The fourth factor is random errors in measurement, which includes the mechanical vibration of camera installation, air turbulence, and illumination disturbance at the test site. The fifth factor is the transition error between each coordinate system. Such errors can be represented by δ_r and δ_Δ respectively. The error factors mentioned above do not relate to each other, therefore, a single light spot's position error can be expressed as

$$\begin{cases}\delta_{px}=\delta_{py}=\sqrt{\delta_l^2+\delta_c^2+\delta_t^2+\delta_r^2+\delta_\Delta^2}\\ \delta_{pZ}=\sqrt{\delta_s^2+\delta_\Delta^2}\end{cases}. \tag{8}$$

According to the error analysis of light spots hereinbefore, we can set matrices D_0 and D_t for attitude, E_0 and E_t for disturbance error, and then

$$(C+E_c)\cdot(D_0+E_0)=D_t+E_t, \tag{9}$$

$$E_c=E_t\cdot(D_0+E_0)^{-1}-D_t\cdot\left[I-\left(I+E_0^{-1}\cdot D_0\right)^{-1}\right]$$

$$=E_t\cdot(D_0+E_0)^{-1}-D_t\cdot\left(I+E_0^{-1}\cdot D_0\right)^{-1}\cdot E_0^{-1}\cdot D_0, \tag{10}$$

where

$$E_0=\begin{bmatrix}\frac{\partial A_{m14}}{\partial x} & \frac{\partial A_{m23}}{\partial x} & \frac{\partial B_m}{\partial x}\\ \frac{\partial A_{m14}}{\partial y} & \frac{\partial A_{m23}}{\partial y} & \frac{\partial B_m}{\partial y}\\ \frac{\partial A_{m14}}{\partial z} & \frac{\partial A_{m23}}{\partial z} & \frac{\partial B_m}{\partial z}\end{bmatrix}\cdot\begin{bmatrix}\delta_x & 0 & 0\\ 0 & \delta_y & 0\\ 0 & 0 & \delta_z\end{bmatrix},$$

$$E_t=\begin{bmatrix}\frac{\partial A'_{m14}}{\partial x} & \frac{\partial A'_{m23}}{\partial x} & \frac{\partial B'_m}{\partial x}\\ \frac{\partial A'_{m14}}{\partial y} & \frac{\partial A'_{m23}}{\partial y} & \frac{\partial B'_m}{\partial y}\\ \frac{\partial A'_{m14}}{\partial z} & \frac{\partial A'_{m23}}{\partial z} & \frac{\partial B'_m}{\partial z}\end{bmatrix}\cdot\begin{bmatrix}\delta'_x & 0 & 0\\ 0 & \delta'_y & 0\\ 0 & 0 & \delta'_z\end{bmatrix}.$$

According to the theories in matrix analysis, we can get

$$\frac{\|E_c\|}{\|C\|}\le\frac{\left\|D_0^{-1}\right\|}{1-\left\|D_0^{-1}\right\|\cdot\|E_0\|}\cdot\left(\frac{\|E_t\|}{\|C\|}+\|E_0\|\right)$$

$$\le\frac{\kappa(D_0)}{1-\kappa(D_0)\frac{\|E_0\|}{\|D_0\|}}\left(\frac{\|E_t\|}{\|D_t\|}+\frac{\|E_0\|}{\|D_0\|}\right), \tag{11}$$

Table 1. Comparison between Input and Measured Values

Input Value (deg.)			Measured Value (deg.)			Measurement Error (deg.)		
Yaw	Roll	Pitching	Yaw	Roll	Pitching	Yaw	Roll	Pitching
−10	−10	−10	−10.0135	−9.9801	−10.0335	−0.0135	0.0099	−0.0335
−8	−8	−8	−8.0121	−7.9809	−8.0261	−0.0121	0.0091	−0.0261
−6	−6	−6	−6.0090	−5.9913	−6.0188	−0.0090	0.0067	−0.0188
−4	−4	−4	−4.0074	−3.9844	−4.0161	−0.0074	0.0056	−0.0161
−2	−2	−2	−2.0042	−1.9876	−2.0088	−0.0042	0.0024	−0.0088
0	0	0	−0.0014	0.0012	−0.0012	−0.0014	0.0012	−0.0012
2	2	2	1.9979	2.0027	1.9933	−0.0021	0.0027	−0.0067
4	4	4	3.9942	4.0047	3.9852	−0.0053	0.0047	−0.0148
6	6	6	5.9928	6.0068	5.9798	−0.0072	0.0068	−0.0202
8	8	8	7.9892	8.0080	7.9777	−0.0108	0.0080	−0.0223
10	10	10	9.9851	10.0082	9.9715	−0.0149	0.0082	−0.0285

where $\|\bullet\|$ represents the norm of matrix, $\kappa(D_0) = \|D_0\| \cdot \|D_0^{-1}\|$.

After getting the maximum relative error of transition matrix C, it can be confirmed that the relative error of any elements in transition matrix C is smaller than that. In this way, we can further estimate the maximum relative error of each attitude angle.

The simulation test uses a triaxial turntable as test target. The laser cooperative target is installed on the turntable (from outer ring to inner ring: yaw axis, roll axis, and pitching axis). Two projection screens are set up at both sides of the test site (the distance between screens is 13 m), and two high-speed complementary metal oxide semiconductor (CMOS) cameras (exposure frequency 1/10000 s, 400 frames/s, resolution 1280×1024 pixels) are located besides each screen. Laser Tracker 3D (Automated Precision, Inc., USA) is applied for global calibration. The turntable is located at the center of test site. Only static test is adopted in the simulation test to eliminate the error caused by the vibration of turntable. After recording the image of light spots at the initial position, let the turntable start to rotate point-by-point by a given degree within $\pm 10°$, meanwhile use cameras to capture static images and analyze the measuring effectiveness. Table 1 gives the results recorded during the point-by-point movement of the turntable's three axes. The test results have certain accumulative errors, with the straightness error of laser beams included, which is more vulnerable to angle influence. Each axis has certain error when it is back to its initial position due to the simulation turntable itself has certain errors in installation and rotary. Pitching angle has the lowest measurement accuracy among all attitude angles, because light spots' position variation is relatively small along with the change of pitching angle. Increasing the angle between two laser beams projected by cooperative targets can increase the measurement accuracy of pitching angle but reduce the whole system's measurement range. The simulation test results indicate that measurement error can be limited within $3'$ while the rotation angles of three axes are within $\pm 10°$.

In summary, this work presents a mathematical model of light-spot imaging based on image sequences, which can be applied for the measurement of a close range aircraft's external 3D attitude parameters. On the basis of this model, we analyzed the error sources that may affect the accuracy, and further estimated its maximum relative error mathematically. The system accuracy is affected by the global calibration accuracy, the screen plane errors as well as the processing error of the laser cooperative target. Moreover, the test site has to be arranged in advance according to the range of variation of aircraft attitude. This method needs high-speed mass storage due to the massive data produced in unit time, and it is incapable of real-time processing. These issues require further improvement.

This work was supported by the National Natural Science Foundation of China under Grant No. 50275040. Z. Li's e-mail address is lizhe1978@hit.edu.cn.

References

1. J. Xu, T. Arslan, D. Wang, and Q. Wang, in *Proceedings of the IEEE International Conference on Evolutionary Computation* **12,** 998 (2002).
2. K. Sawada, M. Okihara, and S. Nakamura, Presence **11,** 109 (2002).
3. Q. Yu, X. Sun, and G. Chen, Journal of National University of Defense Technology (in Chinese) **22,** (2) 15 (2000).
4. D. P. McReynolds and D. G. Lowe, IEEE Trans. Pattern Anal. Machine Intell. **18,** 1174 (1996).
5. M. A. Abidi and T. Chandra, IEEE Trans. Pattern Anal. Machine Intell. **17,** 534 (1995).
6. Z. Zhang, G. Su, J. Zhang, and S. Zheng, Geometrics and Information Science of Wuhan University (in Chinese) **29,** 287 (2004).
7. Y. Ding, X. Peng, J. Tian, W. Zhao, A. Li, and X. Zhao, Acta Opt. Sin. (in Chinese) **27,** 451 (2007).
8. M. L. Liu and K. H. Wong, Pattern Recogn. Lett. **20,** 69 (1999).
9. L. Lin and C. Li, Journal of Astronautics (in Chinese) (2) 24 (1994).
10. Q. Xu, D. Ye, and R. Che, Acta Opt. Sin. (in Chinese) **28,** 81 (2008).
11. H. Malm and A. Heyden, IEEE Trans. Robot. **22,** 322 (2006).
12. Z. Zhang, IEEE Trans. Pattern Anal. Machine Intell. **22,** 1330 (2000).
13. R. Y. Tsai, IEEE J. Robot. Automat. **3,** 323 (1987).